PHYSICAL REVIEW E **90**, 051003(R) (2014)

On the edge of an inverse cascade

Kannabiran Seshasayanan,[1] Santiago Jose Benavides,[2] and Alexandros Alexakis[1,3,*]
[1]*Laboratoire de Physique Statistique, CNRS UMR 8550, École Normale Supérieure, Paris, France, and CNRS, Université Pierre et Marié Curie, Paris, France*
[2]*Physics Department, The University of Texas at Austin, Austin, Texas 78712, USA*
[3]*Université Paris Diderot, Paris 75013, France*
(Received 16 June 2014; published 21 November 2014)

We demonstrate that systems with a parameter-controlled inverse cascade can exhibit critical behavior for which at the critical value of the control parameter the inverse cascade stops. In the vicinity of such a critical point, standard phenomenological estimates for the energy balance will fail since the energy flux towards large length scales becomes zero. We demonstrate this using the computationally tractable model of two-dimensional (2D) magnetohydrodynamics in a periodic box. In the absence of any external magnetic forcing, the system reduces to hydrodynamic fluid turbulence with an inverse energy cascade. In the presence of strong magnetic forcing, the system behaves as 2D magnetohydrodynamic turbulence with forward energy cascade. As the amplitude of the magnetic forcing is varied, a critical value is met for which the energy flux towards the large scales becomes zero. Close to this point, the energy flux scales as a power law with the departure from the critical point and the normalized amplitude of the fluctuations diverges. Similar behavior is observed for the flux of the square vector potential for which no inverse flux is observed for weak magnetic forcing, while a finite inverse flux is observed for magnetic forcing above the critical point. We conjecture that this behavior is generic for systems of variable inverse cascade.

DOI: 10.1103/PhysRevE.90.051003 PACS number(s): 47.27.Cn, 74.40.Gh

In many dynamical systems in nature, energy is transferred to smaller or to larger length scales by a mechanism known as forward or inverse cascade, respectively. In three-dimensional hydrodynamic (HD) turbulence, energy cascades forward from large to small scales, while in two-dimensional (2D) HD turbulence, energy cascades inversely from small scales to large scales [1,2]. There are some examples, however, that have a mixed behavior, such as fast rotating fluids, stratified flows, conducting fluids in the presence of strong magnetic fields, or flows in constrained geometry [3–10]. In these examples, the injected energy cascades both forward and inversely in fractions that depend on the value of a control parameter μ (rotation rate, magnetic field, or aspect ratio). In rotating flows, for example, when the rotation is weak, the behavior of the flow is similar to isotropic turbulence and energy cascades forward. As the rotation rate is increased, variations along the direction of rotation are suppressed and the flow starts to become quasi-2D. Eventually, when rotation is strong enough, the two-dimensional component of the flow dominates and energy starts to cascade inversely to the large scales. This behavior has also been observed in experimental setups [11–14] as well as in atmospheric boundary layers [15]. This dual cascade behavior is neither restricted to quasi-2D flows nor to the cascade of energy. It is also observed in wave systems, such as surface waves [16], elastic waves [17], and quantum fluids [18]. The variance of a passive scalar is also shown to display a change of direction of cascade when the compressibility of the flow or its geometry vary [10,19]. Finally, in turbulent dynamo flows, the flux of magnetic helicity changes direction depending on the sign of the kinetic helicity [20,21]. Thus, the transition from forward to inverse cascade by the variation of a control parameter μ is a common property for many out-of-equilibrium systems.

This transition can occur either in a smooth way or by a bifurcation at a critical value μ_c of the control parameter for which the transition from forward to inverse cascade begins. Such a transition differs from the regular scenario of bifurcation from laminar to turbulent flows since in this case the system transitions from one fully turbulent state to another fully turbulent state, making regular expansions nonapplicable. This behavior more closely resembles phase transitions in equilibrium statistical mechanics where an order parameter (for instance, the magnetization for a system of spins) deviates continuously from zero but with discontinuous derivatives and its susceptibility theoretically diverging at the critical point. The order parameter then depends on the distance from the critical point as a power law. Following this analogy, we also expect that for the out-of-equilibrium systems, the energy flux of the inverse cascade will depend on the distance from the critical point μ_c as a power law $\Pi_E \propto (\mu - \mu_c)^\gamma$.

The ideas of critical transitions in turbulence were introduced in [22–24], where a transition from forward to inverse cascade was considered to occur at a critical fractal dimension D with $2 < D < 3$. These ideas were pursued with the use of eddy-damped quasinormal Markovian (EDQNM) models [22] and shell models [25,26], while more recently fractal dimensional turbulence has been modeled by decimated Navier-Stokes models [27].

In this work, we try to demonstrate the idea of an inverse cascade near criticality for a realistic model: the two-dimensional incompressible magnetohydrodynamics (MHD) in a double periodic square domain of size $2\pi L$. As we describe below, this system has a variable inverse cascade of energy. It has the advantage that numerically it can be studied at low computational cost due to its low

*Corresponding author: alexakis@lps.ens.fr

dimensionality and it can be realized also in laboratory experiments. The dynamical equations for the system can be written in terms of the vorticity $\omega = \mathbf{e}_z \cdot \nabla \times \mathbf{u}$ (where $\mathbf{u}$ is the velocity field) and the vector potential a of the magnetic field $\mathbf{b} = \nabla \times (\mathbf{e}_z a)$. They are given by

$$\begin{aligned} \partial_t \omega + \mathbf{u} \cdot \nabla \omega &= \mathbf{b} \cdot \nabla j + \nu^+ \Delta^n \omega + \nu^- \Delta^{-m} \omega + \phi_\omega, \\ \partial_t a + \mathbf{u} \cdot \nabla a &= +\eta^+ \Delta^n a + \eta^- \Delta^{-m} a + \phi_a, \end{aligned} \tag{1}$$

where $\mathbf{e}_z$ is the unit vector normal to the plane, and $j = \mathbf{e}_z \cdot \nabla \times \mathbf{b}$. ϕ_ω and ϕ_a introduce the mechanical force $\mathbf{F_u} = -\Delta^{-1} \nabla \times (\mathbf{e}_z \phi_\omega)$ and the magnetic force $\mathbf{F_b} = \nabla \times (\mathbf{e}_z \phi_a)$ that inject energy in the system at the scale k_f^{-1}. In particular, we have chosen $\phi_\omega = 2 f_0 k_f \cos(k_f x) \cos(k_f y)$ and $\phi_a = \mu f_0 k_f^{-1} \sin(k_f x) \sin(k_f y)$. Therefore, $\mu = \|\mathbf{F_b}\|/\|\mathbf{F_u}\|$ expresses the ratio of magnetic to mechanical forcing. Energy is removed from the system by the terms proportional to ν^+ and η^+ in the small scales and by ν^- and η^- in the large scales. The indexes m,n give the order of the Laplacian used. The physically motivated values are $n = 1$ and $m = 0$; however, to obtain a larger inertial range, we chose $n = m = 2$. For all runs, we have fixed $\nu^+ = \eta^+$ and $\nu^- = \eta^-$.

With these choices, we are left with four control parameters. We have a Reynolds number for the forward energy cascade, $\mathrm{Re}^+ \equiv (f_0^{1/2} k_f^{1/2-2n})/|\nu^+|$, a Reynolds number for the inverse energy cascade, $\mathrm{Re}^- \equiv (f_0^{1/2} k_f^{1/2+2m})/|\nu^-|$, the ratio of the forcing length scale to the box size $k_f L$, and $\mu = \|\mathbf{F_b}\|/\|\mathbf{F_u}\|$. The last parameter controls the transition from an inverse cascade to a direct cascade.

The system in the absence of forcing and dissipation conserves two positive-definite quadratic quantities: the total energy $E = \frac{1}{2}\langle \mathbf{u^2} + \mathbf{b^2} \rangle$ and the square vector potential $A = \frac{1}{2}\langle a^2 \rangle$, where $\langle \cdot \rangle$ indicates the spatial average. In the absence of any external magnetic field or a magnetic source ϕ_a, any magnetic field fluctuations that exist at $t = 0$ will die out (due to the antidynamo theorem of 2D flows [28]) and the system will reduce to ordinary 2D fluid turbulence with an inverse cascade for energy [2] and a forward cascade of A that acts like the variance of a passive scalar [29]. If, however, a magnetic force $\mathbf{F_b}$ exists (and is sufficiently strong), then the flow will sustain magnetic field fluctuations and become magnetic dominated with a forward energy cascade [30] and an inverse cascade of A [31,32].

The flux of energy at any wave number k is defined as

$$\Pi_E(k) \equiv \langle \mathbf{u}_k^<(\mathbf{u} \cdot \nabla \mathbf{u} - \mathbf{b} \cdot \nabla \mathbf{b}) + \mathbf{b}_k^<(\mathbf{u} \cdot \nabla \mathbf{b} - \mathbf{b} \cdot \nabla \mathbf{u}) \rangle, \tag{2}$$

while $\Pi_A(k) \equiv \langle a_k^< (\mathbf{u} \cdot \nabla a) \rangle$ defines the flux of the square vector potential [30]. Here, $g_k^<$ represents the filtered field g so that only the Fourier modes $\mathbf{k}$ satisfying $|\mathbf{k}| \leqslant k$ have been kept. The dissipation rate of energy at the small scales is defined in terms of the Fourier components of the two fields $\tilde{\mathbf{u}}_\mathbf{k}, \tilde{\mathbf{b}}_\mathbf{k}$ as

$$\epsilon_E^+ \equiv |\nu^+| \sum_{\mathbf{k} \neq \mathbf{0}} |\mathbf{k}|^{2n} (|\tilde{\mathbf{u}}_\mathbf{k}|^2 + |\tilde{\mathbf{b}}_\mathbf{k}|^2), \tag{3}$$

TABLE I. Numerical parameters of the direct numerical simulations (DNS). For all runs, $\mathrm{Re}^+ = 1400$. T expresses the typical duration of the runs in units of $1/\sqrt{f_0 k_f}$. In most cases, a duration of $T = 100$ was sufficient to obtain a good average of ϵ_E^- and ϵ_A^-; smaller resolution simulations were run further in time to obtain statistics on the behavior of the flux fluctuations.

$k_f L$	8	16	32	64
N	512	1024	2048	4096
Re^-	2.3×10^4	7.4×10^5	2.3×10^7	7.6×10^8
T	2000	600	342	100

while in the large scales it is defined as

$$\epsilon_E^- \equiv |\nu^-| \sum_{\mathbf{k} \neq \mathbf{0}} |\mathbf{k}|^{-2m} (|\tilde{\mathbf{u}}_\mathbf{k}|^2 + |\tilde{\mathbf{b}}_\mathbf{k}|^2). \tag{4}$$

Similarly, we define the dissipation of A,

$$\epsilon_A^+ \equiv |\nu^+| \sum_{\mathbf{k} \neq \mathbf{0}} |\mathbf{k}|^{2n} |\tilde{a}_\mathbf{k}|^2 \quad \text{and} \quad \epsilon_A^- \equiv |\nu^-| \sum_{\mathbf{k} \neq \mathbf{0}} |\mathbf{k}|^{-2m} |\tilde{a}_\mathbf{k}|^2. \tag{5}$$

The dissipation rates at the large scales ϵ_E^- and ϵ_A^- provide a measure of the strength of the inverse cascade. In the infinite Re^- limit, ϵ_E^- and ϵ_A^- will be nonzero if and only if an inverse cascade exists. For any finite value of Re^-, however, some weak large scale dissipation will exist due to the finite value of the dissipation coefficients ν^-,η^-. To investigate the large Re^- limit, the following procedure was followed: for fixed $\mathrm{Re}^\pm$ and $k_f L$, simulations were performed for different values of μ varying from 0 to 1. The flow was simulated using a standard pseudospectral code [33]. The simulations were run long enough in time so that a steady state is reached and long time averages can be performed. Then, keeping Re^+ fixed, we increased $k_f L$ and Re^- and a new series of simulations was performed varying μ in the same range. Re^- was chosen as large as possible so that a clean inertial range was obtained, but sufficiently small so that no large scale condensate formed at the large scales. The values of the control parameters are given in Table I.

Figure 1 presents the large scale dissipation rates ϵ_E^- and ϵ_A^- normalized by the total injection rates $\epsilon_E = \epsilon_E^- + \epsilon_E^+$ and $\epsilon_A = \epsilon_A^- + \epsilon_A^+$ as a function of μ. The different colors and symbols indicate the different values of $k_f L$ used. For small values of μ, the system behaves like HD flow with an inverse cascade of energy indicated by the fact that almost all of the injected energy is dissipated in the large scales $\epsilon_E^-/\epsilon_E \simeq 1$. At the same time, no inverse cascade of A is observed since $\epsilon_A^-/\epsilon_A \simeq 0$. For $\mu \simeq 1$, on the other hand, the system behaves like an MHD flow with no inverse cascade of energy $\epsilon_E^-/\epsilon_E \simeq 0$ but an inverse cascade of A, $(\epsilon_A^-/\epsilon_A \simeq 1)$. For intermediate values of μ, the energy and square vector potential are dissipated both at large and small scales at fractions that depend on μ, with the inverse cascade of energy decreasing with μ and the inverse cascade of A increasing with μ.

Around $\mu \simeq 0.22$, the inverse cascade of energy ends and, at $\mu \simeq 0.25$, the inverse cascade of A begins. The two cascades thus seem to have different critical values. The transition is less sharp for small values of $k_f L$. However, as the domain size

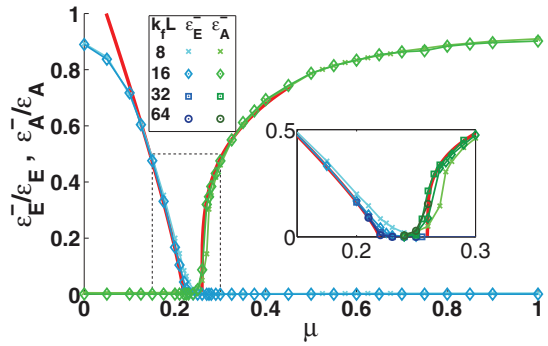

FIG. 1. (Color online) Normalized energy dissipation in the large scales ϵ_E^-/ϵ_E and normalized square vector potential dissipation ϵ_A^-/ϵ_A as a function of μ for different values of $k_f L$ (as indicated by the table in the figure). Inset: A zoom of the same data close to the critical point. The red lines show the fitting curves $(\mu_c - \mu)^{\gamma_E}$ and $(\mu - \mu_c)^{\gamma_A}$.

$k_f L$ is increased, the curves converge to a sharp transition and the two transition points approach each other. This can be seen more clearly at the inset, where a closeup at the critical point is shown. Due to the long time to reach saturation in the presence of inverse cascades, the large $k_f L$ cases (that also required the largest resolutions) were limited only to values of μ close to the critical points.

Both dissipation rates scale as power laws $\epsilon_E^- \propto (\mu_c - \mu)^{\gamma_E}$ and $\epsilon_A^- \propto (\mu - \mu_c)^{\gamma_A}$, with a best fit leading to $\gamma_E \simeq 0.82$ and $\gamma_A \simeq 0.27$. However, not being able to determine precisely the value of μ_c significantly limits the accuracy of these measurements. Furthermore, the exact location of μ_c was also found to depend on the value of Re^+ caused by the dependence of magnetic energy on Re^+. Besides the energy flux, other quantities also showed power-law behaviors. A full presentation of the results of the 2D-MHD system will be reported in a lengthier report. Here we focus on the more general features of the cascade transition scenario.

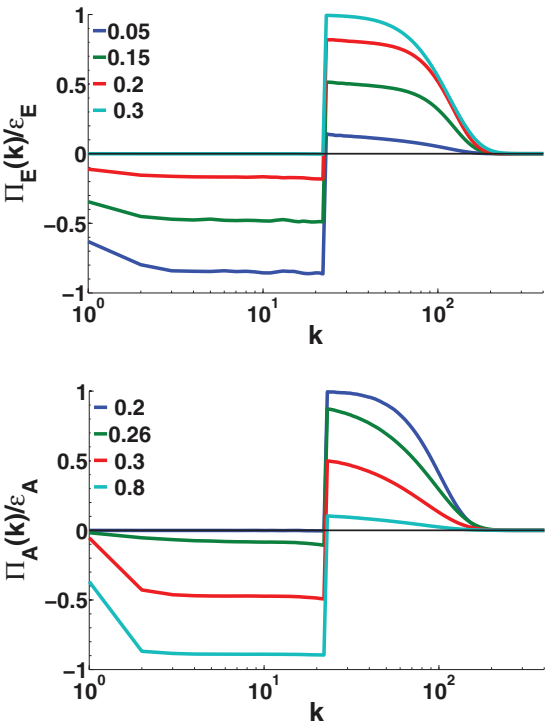

FIG. 2. (Color online) The energy flux $\Pi_E(k)$ (top panel) and the flux of the square vector potential $\Pi_A(k)$ (lower panel) for different values of μ around the critical point and $k_f L = 16$.

The cascade transition can be seen in the plots of the two normalized fluxes $\Pi_E(k)/\epsilon_E$ and $\Pi_A(k)/\epsilon_A$, shown for various values of μ in Fig. 2. The two fluxes remain constant in k for a wide range of wave numbers. As the parameter μ is varied, the flux varies from 0 to -1 (in the range $k < k_f$) and from 0 to $+1$ (in the range $k > k_f$). At intermediate values of $0 < \mu < \mu_c$, part of the energy cascades to small scales and part cascades to large scales, and similarly for A in the range $\mu > \mu_c$. We note that this behavior is met in other systems of variable cascade [3–10] and should be reproduced by any theoretical modeling (see, e.g., [34]).

We emphasize the role of the flux fluctuations close to the critical value. The inset in Fig. 3 shows the time averaged flux $\Pi_E(k)$ with the dark blue line, while with the light cyan lines the instantaneous flux $\Pi_E(t,k)$ is plotted at various instances of time. The instantaneous flux is not constant in k; on the contrary, it fluctuates, taking both positive and negative values. The amplitude of the fluctuations of the flux greatly exceed the averaged flux. In fact, as Fig. 3 shows, the relative amplitude of the fluctuations σ_E and σ_A (standard deviation from the mean value) to the averaged value diverges as the critical point is approached.

Finally, we note the effect of μ on the distribution of energy in scale space. Dimensional phenomenological arguments predict that the energy spectra E_u and E_b of the two fields will follow different power laws in the two extreme limits. In the large scales ($k < k_f$) for weak magnetic forcing, we expect the scaling $E_u(k) \sim k^{-5/3}$ for the kinetic energy spectrum and $E_b \sim k^3$ if we assume equipartition of A among all Fourier modes. For strong magnetic forcing, we expect

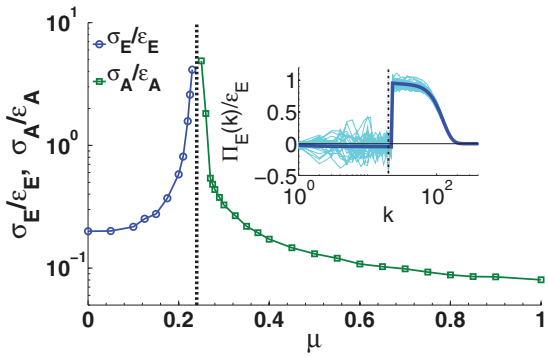

FIG. 3. (Color online) Inset: The instantaneous energy flux $\Pi_E(t,k)$ with cyan lines for various times t and the time averaged energy flux $\Pi_E(k)$ with the dark blue line for $\mu = 0.21$ and $k_f L = 16$. The main figure shows the variance of the energy flux $\sigma_E = \langle[\Pi_E(t,k) - \Pi_E(k)]^2\rangle^{1/2}$ and the variance of the square vector potential flux σ_A normalized by the large scale dissipations. The fluxes were evaluated at k slightly smaller than the forcing wave number indicated by the vertical dashed line in the inset.

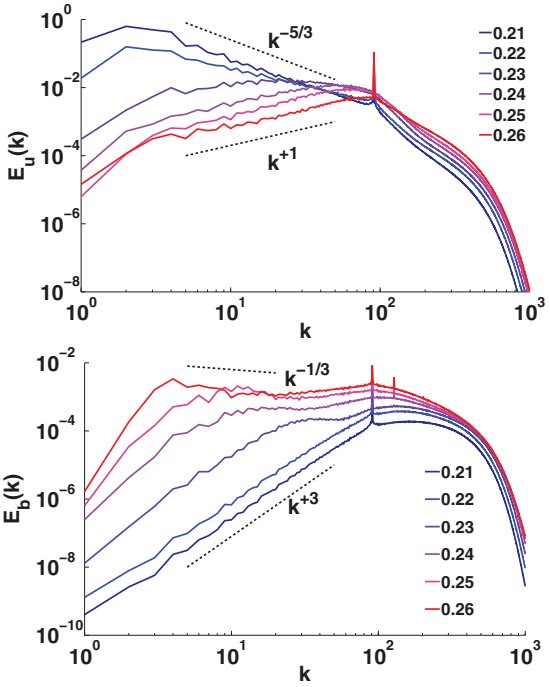

FIG. 4. (Color online) Kinetic energy spectra (top panel) and magnetic energy spectra (bottom panel) for $k_f L = 64$ and different values of μ varying from 0.21 to 0.26.

the scaling $E_u \sim E_b \sim k^{-1/3}$ due to the constant flux of A. These exponents, however, have been criticized before in the literature [35] and have been shown to be sensitive to dissipation parameters. Figure 4 shows the kinetic energy spectra and the magnetic energy spectra for different values of the parameter μ varying from $\mu = 0.21$ to $\mu = 0.26$ and $k_f L = 64$. It is clear that as μ crosses the critical value μ_c, the slope of the kinetic energy spectrum varies from a value close to $-5/3$ to a value that could be interpreted as $+1$, implying equipartition of kinetic energy in all modes. The slope of the magnetic energy spectrum, on the other hand, decreases from the positive $+3$ value to a value close to $-1/3$. Here, thus, we give an alternative interpretation of the variable exponent that has been measured in the literature for 2D-MHD that the exponent can vary due to the transition from 2D-HD to 2D-MHD. We note that such variation of the spectral exponent of the inverse cascade has also been observed in rotating turbulence [3]. Of course, we note that we have only limited inertial range and what appears as a variable spectral index could, in fact, be a smooth transition at some transition wave number from the $k^{-5/3}$ regime to the $k^{-1/3}$ regime.

Concluding, we have demonstrated that the transition from 2D-HD to 2D-MHD by varying the magnetic forcing amplitude has a critical behavior. We expect that this is not a unique property of 2D-MHD but can also be observed in some of the other systems that were mentioned in the introduction. As far as we know, there is no quantitative theory that describes these transitions. Thus, they pose new questions and open new venues for the studies of out-of-equilibrium systems and turbulence.

This work was granted access to the high-performance-computing resources of GENCI-CINES (Project No. x2014056421) and MesoPSL financed by the Region Ile de France and the project EquipMeso (Reference No. ANR-10-EQPX-29-01). K.S. acknowledges support from the LabEx ENS-ICFP: ANR-10-LABX-0010/ANR-10-IDEX-0001-02 PSL. S.J.B. acknowledges support from the College of Natural Sciences Summer Research Abroad Scholarship, University of Texas at Austin.

[1] U. Frish, *Turbulence: The Legacy of A. N. Kolmogorov* (Cambridge University Press, Cambridge, 1995).
[2] G. Boffetta and R. E. Ecke, Ann. Rev. Fluid Mech. **44**, 427 (2012).
[3] A. Sen, P. D. Mininni, D. Rosenberg, and A. Pouquet, Phys. Rev. E **86**, 036319 (2012).
[4] E. Deusebio, G. Boffetta, E. Lindborg, and S. Musacchio, Phys. Rev. E **90**, 023005 (2014).
[5] A. Alexakis, Phys. Rev. E **84**, 056330 (2011).
[6] K. S. Reddy and M. K. Verma, Phys. Fluids **26**, 025109 (2014).
[7] A. Sozza, G. Boffetta, P. Muratore-Ginanneschi, and S. Musacchio, arXiv:1405.7824.
[8] A. Pouquet and R. Marino, Phys. Rev. Lett. **111**, 234501 (2013).
[9] R. Marino, P. D. Mininni, D. Rosenberg, and A. Pouquet, Eur. Phys. Lett. **102**, 44006 (2013).
[10] A. Celani, S. Musacchio, and D. Vincenzi, Phys. Rev. Lett. **104**, 184506 (2010).
[11] L. M. Moubarak and G. Y. Antar, Exp. Fluids **53**, 1627 (2012).
[12] D. Byrne, H. Xia, and M. Shats, Phys. Fluids **23**, 095109 (2011).
[13] H. Xia, D. Byrne, G. Falkovich, and M. Shats, Nat. Phys. **7**, 321324 (2011).
[14] M. Shats, D. Byrne, and H. Xia, Phys. Rev. Lett. **105**, 264501 (2010).
[15] D. Byrne and J. A. Zhang, Geophys. Res. Lett. **40**, 1439 (2013).
[16] L. V. Abdurakhimov, I. A. Remizov, A. A. Levchenko, G. V. Kolmakov, and Y. V. Lvov, arXiv:1404.1111.
[17] B. Miquel, A. Alexakis, Ĉ. Josserand, and N. Mordant, Phys. Rev. Lett. **111**, 054302 (2013).
[18] A. N. Ganshin, V. B. Efimov, G. V. Kolmakov, L. P. Mezhov-Deglin, and P. V. E. McClintock, Phys. Rev. Lett. **101**, 065303 (2008).
[19] K. Gawędzki and M. Vergassola, Physica D **138**, 63 (2000).
[20] A. Alexakis, P. D. Mininni, and A. Pouquet, Astrophys. J. **640**, 335 (2006).
[21] S. K. Malapaka and W.-Ch. Müller, Astrophys. J. **778**, 21 (2013).
[22] U. Frisch, M. Lesieur, and P. L. Sulem, Phys. Rev. Lett. **37**, 895 (1976).
[23] J. D. Fournier and U. Frisch, Phys. Rev. A **17**, 747 (1978).
[24] V. Yakhot, Phys. Rev. E **63**, 026307 (2001).
[25] T. L. Bell and M. Nelkin, Phys. Fluids **20**, 345 (1977).
[26] P. Giuliani, M. H. Jensen, and V. Yakhot, Phys. Rev. E **65**, 036305 (2002).

[27] U. Frisch, A. Pomyalov, I. Procaccia, and S. S. Ray, Phys. Rev. Lett. **108**, 074501 (2012).
[28] Y. B. Zeldovich, Sov. Phys. J. Exp. Theor. Phys. **4**, 460 (1957).
[29] G. K. Batchelor, J. Fluid Mech. **5**, 113133 (1959).
[30] D. Biskamp, *Magnetohydrodynamic Turbulence* (Cambridge University Press, Cambridge, 2003).
[31] A. Pouquet, J. Fluid Mech. **88**, 1 (1978).
[32] D. Fyfe and D. Montgomery, J. Plasma Phys. **16**, 181 (1976).
[33] D. O. Gomez, P. D. Mininni, and P. Dmitruk, Phys. Scr. T **116**, 123 (2005).
[34] G. Boffetta, F. De Lillo, and S. Musacchio, Phys. Rev. E **83**, 066302 (2011).
[35] D. Banerjee and R. Pandit, Phys. Rev. E **90**, 013018 (2014).